Bacterial mass transport and adhesion using macroscopic fluorescense imaging

Li, Jiuyi

Chapter 2

Analysis of the contribution of sedimentation to bacterial mass transport in a parallel plate flow chamber

Reproduced with permission of Elsevier b.v. from: J. Li, H. J Busscher, W. Norde, J. Sjollema, (2011) *Colloids and Surfaces B: Biointerfaces*, **84**, 76–81.

ABSTRACT

In order to investigate bacterium-substratum interactions, understanding of bacterial mass transport is necessary. Comparisons of experimentally observed initial deposition rates with mass transport rates in parallel-plate-flow-chambers (PPFC) predicted by convective-diffusion yielded deposition efficiencies above unity, despite electrostatic repulsion. It is hypothesized that sedimentation is the major mass transport mechanism in a PPFC. The contribution of sedimentation to the mass transport in a PPFC was experimentally investigated by introducing a novel microscopy-based method. First, height-dependent bacterial concentrations were measured at different times and flow rates and used to calculate bacterial sedimentation velocities. For *Staphylococcus aureus* ATCC 12600, a sedimentation velocity of 240 $\mu m\ h^{-1}$ was obtained. Therewith, sedimentation appeared as the predominant contribution to mass transport in a PPFC. Also in the current study, deposition efficiencies of *S. aureus* ATCC 12600 with respect to the Smoluchowski-Levich solution of the convective-diffusion equation were four-to-five fold higher than unity. However, calculation of deposition efficiencies with respect to sedimentation were below unity and decreased from 0.78 to 0.36 when flow rates increased from 0.017 to 0.33 $cm^3\ s^{-1}$. The proposed analysis of bacterial mass transport processes is simple, does not require additional equipment and yields a more reasonable interpretation of bacterial deposition in a PPFC.

INTRODUCTION

Bacterial adhesion occurs to virtually all surfaces exposed to an aqueous environment and leads to the subsequent growth of a biofilm. Biofilms can be found nearly everywhere, such as in groundwater, pipelines in waterworks, wastewater treatment plants, on the surfaces of heat exchanger plates and biomedical devices, and on ship hulls [1-5]. Flow displacement systems are widely used to study bacterial adhesion to surfaces [6-10] as they allow control of hydrodynamic conditions, including shear rates and mass transport.

Bacterial mass transport in flow displacement systems is generally established by a combination of convection, diffusion and sedimentation. Previous studies on bacterial mass transport in a parallel plate flow chamber (PPFC) have adopted the Smoluchowski-Levich (SL) approximation of the two-dimensional convective-diffusion equation to predict mass transport in the absence of gravitational, colloidal and hydrodynamic interactions [11] to either the top or bottom plate of a chamber [12-14]. In the SL approximation, it is assumed that the substratum surface acts as a perfect sink (i.e. every particle or bacterium that arrives at the surface adheres irreversibly). Accordingly, the ratio between the experimentally observed initial deposition rate, j_0, and the bacterial mass transport rate calculated by SL approximation, j_0^*, indicates the fraction of bacteria arriving at the surface that manages to adhere successfully under the influence of the interaction forces between arriving bacteria and the substratum surface. For this reason, the ratio j_0/j_0^* is also referred to as “deposition efficiency”.

Electrostatic repulsion usually exists between bacterial cell surfaces and most substratum surfaces [15, 16], which negates the assumption made in the SL approximation that the substratum surface should act as a perfect sink. Hence,

deposition efficiencies with respect to the SL approximation should be smaller than unity. However, values in excess of unity have been reported for different bacterial strains and species. *Streptococcus cricetus* showed a high deposition efficiency of almost 2 to the bottom polymethylmethacrylate plate of a PPFC [12], while also *Streptococcus thermophlius* B to the bottom glass plate of a PPFC had a deposition efficiency in excess of unity [13]. Deposition efficiencies of six coagulase-negative staphylococcal strains to negatively charged acrylate bottom plates were as high as 1.4 [14]. Deposition efficiencies in excess of unity have been largely attributed to the complex structural and chemical nature of bacterial cell surfaces and it has even been envisaged that nanoscopic surface appendages protruding from bacterial cell surfaces penetrate the energy barrier between two negatively charged surfaces to give strong primary minimum adhesion. However, these explanations are largely hypothetical, while a much more simple explanation might be that the mass transport rate as derived from the SL approach with respect to which the deposition efficiency is calculated, underestimates the actual mass transport rate towards the substratum.

Therefore, in order to gain a more comprehensive understanding of bacterial mass transport in a PPFC we present a new microscopy-based experimental method to determine the contribution of sedimentation to bacterial mass transport. The method is illustrated for a staphylococcus strain, but is equally applicable to other bacterial strains as well as to inert colloidal particles and does not require additional equipment.

MATERIALS AND METHODS

Bacterial strain and culture conditions

Staphylococcus aureus ATCC 12600 used in this study was physico-chemically characterized previously [17] and cultured aerobically from a blood agar plate in 10 cm^3 Tryptone Soya Broth (OXOID, Basingstoke, England) at 37°C. After 24 h, several colonies were used to inoculate 200 cm^3 Tryptone Soya Broth for 16 h at 37°C, and harvested for use. Bacteria were pelleted by centrifugation (Beckman J2-MC centrifuge, Beckman Coulter, Inc. Brea, CA, USA) for 5 min at 6500 rpm via a JA14 rotor (4000 x g) and resuspended in 10 cm^3 PBS (5 mM K_2HPO_4, 5 mM KH_2PO_4, 0.15 M NaCl, pH 7.0). Centrifugation was done twice in order to remove all traces of growth medium. To break bacterial aggregates, sonication at 30 W (Vibra Cell Model 375, Sonics and Materials Inc., Danbury, CT, USA) was applied (3 times 10 s), while cooling in an ice/water bath. Finally, bacteria were resuspended in PBS to a concentration of 3×10^8 cm^{-3}, as determined in a Bürker-Türk counting chamber.

Substratum surface and parallel plate flow chamber

Glass slides (7.6×2.6×0.1 cm, Menzel-Glaser, Menzel GmbH & Co KG, Germany) constituted the top and bottom plates of the PPFC. Prior to use, slides were sonicated for 3 min in 2% RBS35 (Omnilabo International BV, The Netherlands) followed by thorough rinsing with tap water, demineralized water, methanol, tap water and finally demineralized water again to obtain a hydrophilic surface with a zero degrees water contact angle and a zeta potential by streaming potentials in PBS of -8 mV. The top and bottom glass plates of the chamber on which bacterial adhesion was observed, were placed in the middle of a stainless steel frame (17.5

x 4 cm) and are separated by a Teflon spacer creating a flat channel with a length of 17.5 cm, a height of 0.058 cm and a width of 1.70 cm and a gradually diverging and converging (62 degrees) inlet and outlet region [10,13]. In this configuration, an established flow develops within 2-3 cm from the inlet [10] under laminar conditions. No microscopic flow disturbances were observed due to the steel-glass junction, as judged from the absence of irregular bacterial movements along the surface.

Prior to use, the flow chamber was washed with 2% Extran (Merck, Germany) and rinsed thoroughly with tap water and demineralized water before mounting clean glass slides in the chamber. The flow chamber was positioned between two communicating vessels, and the system was filled with PBS while care was taken to remove all air bubbles. In- and outlet vessels of PBS and bacterial suspension were placed at different heights to create a pulse-free flow by hydrostatic pressure. The difference in fluid level between the vessels was maintained by a roller pump between the vessels to ensure a circulating pulse free flow throughout the duration of the experiment.

Bacterial deposition

Deposition of bacteria was monitored with a phase-contrast microscope (Olympus BH-2) equipped with a 40× ultra long working distance objective (Olympus ULWD-CD Plan 40 PL), connected to a CCD-MXRi camera (Basler A101F, Basler AG, Germany). In order to enhance the signal-to-noise ratio and eliminate moving bacteria from the analysis, 15 images were taken with 0.25 s time intervals, and added to yield a single-time point average. Image analysis was done using

proprietary software based on the Matlab Image Processing Toolkit (The Math Works, MA, USA).

The bacterial suspension was allowed to flow through the flow chamber during 1 h at flow rates of 0.017, 0.033, 0.083, 0.17 or 0.33 $cm^3\ s^{-1}$, corresponding with Reynolds numbers (*Re*), calculated on basis of the hydraulic radius of the channel [10], of 0.95, 1.9, 4.7, 9.5 and 19, respectively. Adhesion was monitored on both top and bottom plates at a distance of 6.2, 8.2 and 11.2 cm from the end of the cylindrical inlet of the stainless steel frame containing the glass slides.

For each flow rate, the number of bacteria adhering per unit area was recorded as a function of time. Adhesion kinetics were expressed in terms of the initial deposition rate j_0 ($cm^{-2}\ s^{-1}$), as determined by linear regression analysis of the initial increase in numbers of adhering bacteria per cm^2 with time. In addition, bacterial deposition assays were carried out under stagnant conditions; i.e. the adhering bacteria were monitored when the silicon tubings, connecting the inlet and outlet of the PPFC, were both closed after 20 min of recirculation (0.17 $cm^3\ s^{-1}$) of a bacterial suspension. All experiments were conducted in six-fold, with at least three separately grown bacterial cultures, i.e. two experiments were carried out with one culture.

The initial deposition rate, $j_{0,}$ was related to the convective-diffusion controlled deposition in a PPFC, calculated using the SL approximation as a solution of the two-dimensional convective diffuson equation,according to [11]

$$j_0^* = \frac{D_\infty c_0}{0.89r}\left[\frac{2}{9}\cdot\frac{bPe}{x}\right]^{1/3} \qquad (1)$$

in which D_∞ is the bacterial diffusion coefficient at large distances from the surface, c_0 is the original number concentration of bacteria in the prepared suspension, r is the bacterial radius, x is the longitudinal distance from the flow chamber entrance, b is the half height of PPFC, and Pe is the dimensionless Peclet number defined as

$$\mathrm{Pe} = \frac{3\mathrm{Qr}^3}{4\mathrm{wb}^3\mathrm{D}_\infty} \tag{2}$$

in which Q is the applied volumetric flow rate.

Bacterial sedimentation rates

In this paper, we present a simple, microscopy-based method to determine the gravitational contribution to bacterial mass transport in a PPFC on the basis of bacterial concentration over the height of the flow channel. First, bacterial concentrations in suspension are measured at different heights in the flow chamber. As a necessary step, the volume of the field of view (FOV) is experimentally determined. Subsequently, the bacterial sedimentation velocity is evaluated under stagnant conditions from the rate of change of bacterial concentration with time in a suspension layer. Finally, the deposition rate to the bottom plate is calculated from the height dependence of the bacterial concentration close to the bottom plate, employing a simple diffusion and sedimentation mass transport equation.

Pulse-free circulation of the bacterial suspension (3×10^8 cm^{-3}) was created by hydrostatic pressure, maintained by a roller pump at the desired flow rate for 20 min to reach a stable hydrodynamic situation, after which the silicon tubings connecting the inlet and outlet of the PPFC were closed simultaneously.

Within 3 min after arresting the flow, bacteria within the layer of fluid in focus, N_i, were counted at different heights, z_i, in the suspension ranging from 15 μm up to 560 μm above the bottom plate. In order to exactly determine the location of the in focus level, the vertical distance between the inward surfaces of the top and bottom glass was determined using a digital micrometer (Absolute ID-C112B, Mitutoyo Corp., Japan). The number of the bacteria in each image was determined by image analysis. For bacterial enumeration, only bacteria which appear as dark objects were considered, as out of focus bacteria form bright objects in phase contrast microscopy. The bacterial concentration, $c(z_i)$, in the layer of fluid at a vertical position z_i, could be expressed as the ratio between the number of bacteria, N_i over the volume of the fluid in focus, being the product of the horizontal area of the FOV, A (corresponding to 3.64×10^{-4} cm^2 under the magnification used), and the depth of field of the microscope objective, d_f, as expressed by the following equation

$$c(z_i) = N_i/(A \cdot d_f) \tag{3}$$

The depth of field is experimentally determined by solving the following equation for d_f:

$$\sum_{i=0}^{n_t} \frac{1}{2} \cdot \left(\frac{N_i + N_{i+1}}{A \cdot d_f}\right) \cdot A \cdot (z_{i+1} - z_i) = 2\, c_0 \cdot A \cdot b \tag{4}$$

As a result of the above procedure, the number of bacteria counted in one image at a given height, can now be transformed into a local bacterial concentration.

Bacterial sedimentation velocity was measured at different heights, z_0 (i.e. 325, 375 and 425 μm above the center of the bottom plate), in the flow channel. In order to reach a stable hydrodynamic condition, recirculation of the bacterial

suspension (3×10^8 cm^{-3}) was maintained for 20 min at 0.17 cm^3 s^{-1}. Immediately after the silicon tubings, connecting the inlet and outlet of the PPFC, were both closed, the initial bacterial concentration height profile, $c(z, t_0)$, was determined at several vertical positions z_t in the fluid between z_0 and the top plate. In addition, the bacterial concentration at z_0, $c(z_0, t)$, was measured as a function of time. Thereafter, another bacterial concentration height profile $c(z, t_e)$ was measured at t_e. The bacterial sedimentation velocity was subsequently calculated based on a mass balance of bacteria, as given by

$$A\int_{z_0}^{z_t} c(z,t_0)dz = A\int_0^{t_e} v_s \cdot c(z_0,t)dt + A\int_{z_0}^{z_t} c(z,t_e)dz \tag{5}$$

in which v_s denotes the bacterial sedimentation velocity. In this equation it is assumed that the effect of diffusional transport can be neglected as compared to the effect of sedimentation, because the diffusion constant of bacteria is low and the concentration gradient in the region between z_t and z_0 is small. Accordingly, v_s can be solved, by transforming the integral equation to finite summations, from

$$v_s = \frac{\sum_{i=1}^{n}[c_i(t_0)+c_{i+1}(t_0)]\cdot(z_{i+1}-z_i) - \sum_{i=1}^{n}[c_i(t_e)+c_{i+1}(t_e)]\cdot(z_{i+1}-z_i)}{2\sum_{j=1}^{m}c_j(z_0)\Delta t} \tag{6}$$

Deposition rates due to sedimentation and diffusion

The height-dependent sedimentation rate, $j_s(z)$, in the PPFC can now be calculated based on the above described experiments as

$$j_s(z) = c(z)\cdot v_s \tag{7}$$

In order to prevent detection of adhering bacteria at $z = 0$, z was taken as close as possible to the surface but never closer than d_f, the depth of field of the microscope objective. The diffusive mass transport rate, $j_D(z)$, within the diffusion boundary layer was calculated from

$$j_D(z) = -D_\infty \frac{\partial c(z)}{\partial z} \tag{8}$$

in which the gradient in bacterial concentration was calculated from the experimentally determined concentration profile at the position z. The theoretical thickness of the diffusion boundary layer, neglecting sedimentation and interaction forces, was calculated according to the following equation [19]

$$\delta_d \approx 5.2\left(\frac{D_\infty \rho_f}{\eta}\right)^{\frac{1}{3}} \cdot \left(\frac{Q \eta x}{2w b \rho_f}\right)^{\frac{1}{2}} \tag{9}$$

in which δ_d is the thickness of the boundary layer for diffusion, η the dynamic viscosity of fluid, ρ_f the mass density of fluid. The values of the parameters adopted for the mass transport indicators in the present study are listed in Table 1.

Table 1. Values for different mass transport parameters used in this study [10,20].

parameter	D_∞	b	w	c_0	η	ρ_s	ρ_f	r
unit	$cm^2\ s^{-1}$	cm	cm	cm^{-3}	Pa s	$g\ cm^{-3}$	$g\ cm^{-3}$	cm
value	3.1×10^{-9}	2.88×10^{-2}	1.7	3×10^{8}	9.3×10^{-4}	1.100	1.013	6×10^{-5}

RESULTS

Bacterial adhesion kinetics

Figs. 1a and b show the number of *S. aureus* ATCC 12600 adhering to the top and bottom plates of the PPFC from which the initial deposition rates, j_0, as summarized in Fig. 1b for the different flow rates applied, can be calculated. The

number of bacteria adhering to the bottom plate increased linearly with time at a flow rate of 0.017 cm^3 s^{-1}, but leveled off for adhesion to the top plate within 600 s (Fig. 1a). The initial deposition rates on the bottom plate were much higher than on the top plate. j_0 on the bottom plate decreased with increasing flow rates, while j_0 on the top plate showed a reverse trend (Fig. 1b).

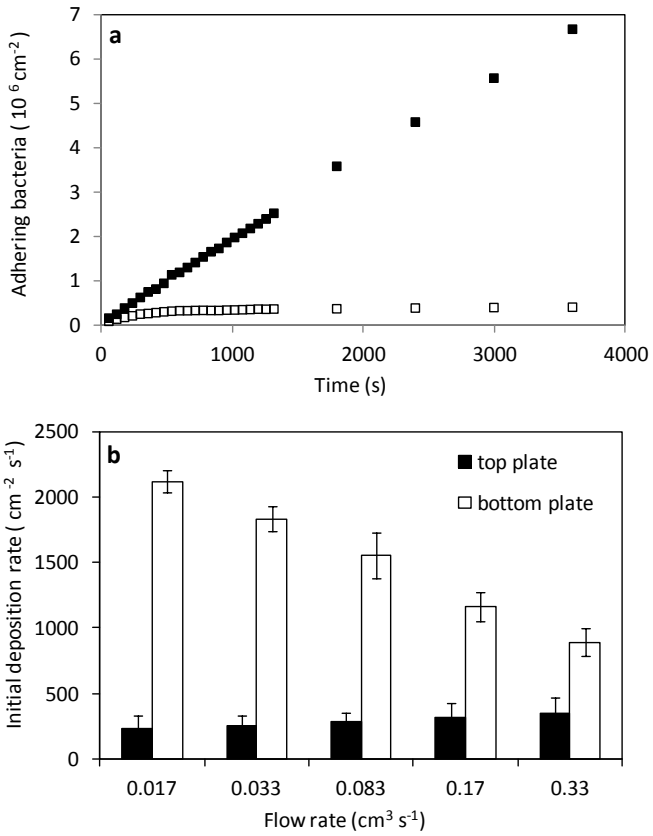

Figure 1. (a) Example of the numbers of *S. aureus* adhering to the top and bottom glass plates of the PPFC as a function of time at a flow rate of 0.017 cm^3 s^{-1}. (b) Initial deposition rates of *S. aureus* to the top and bottom plates of the PPFC at different flow rates and at 6.2cm from the entrance of the PPFC. Error bars indicate the SD over triplicate experiments with separately grown bacteria.

Fig. 2 contains the different experimental and theoretically calculated staphylococcal deposition rates at various distances from the channel entrance. For a given flow rate higher experimental initial deposition rates j_0 were obtained at positions farther downstream (Fig. 2a). Initial deposition rates decreased with increasing flow rates, and, interestingly, the highest initial deposition rate j_0 was observed under stagnant conditions. Opposite to the experimental initial deposition rates, the theoretical bacterial deposition rate, j_0^* calculated using Eq. 1 (Fig. 2b) increased with increasing flow rates. j_0^* was less than 500 cm^{-2} s^{-1} for a flow rate of 0.017 cm^3 s^{-1}, while increasing above 1000 cm^{-2} s^{-1} at a flow rate of 0.33 cm^3 s^{-1}. Lower j_0^* values were calculated for downstream positions in PPFC for a given flow rate than for more upstream positions.

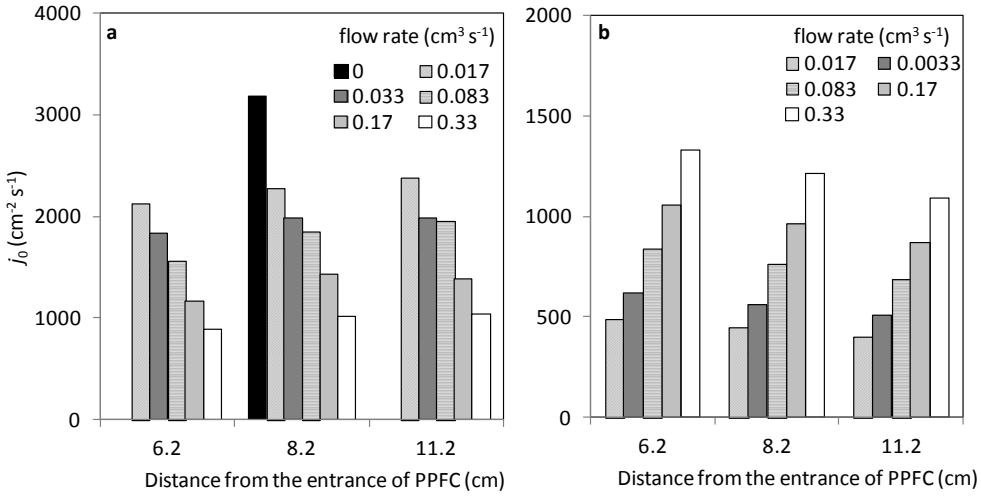

Figure 2. Staphylococcal deposition rates to the bottom plate of a PPFC at different distances from the channel entrance and for different flow rates. (a) Experimental initial deposition rates. (b) Theoretical deposition rates predicted by SL approximation.

Bacterial concentration as a function of height and sedimentation velocities

The depth of field of the objective lens on the microscope was calculated from Eq. 4 to be 14.7 µm, which impedes measurements of bacterial concentrations closer than 15 µm from the top or bottom surfaces of the channel.

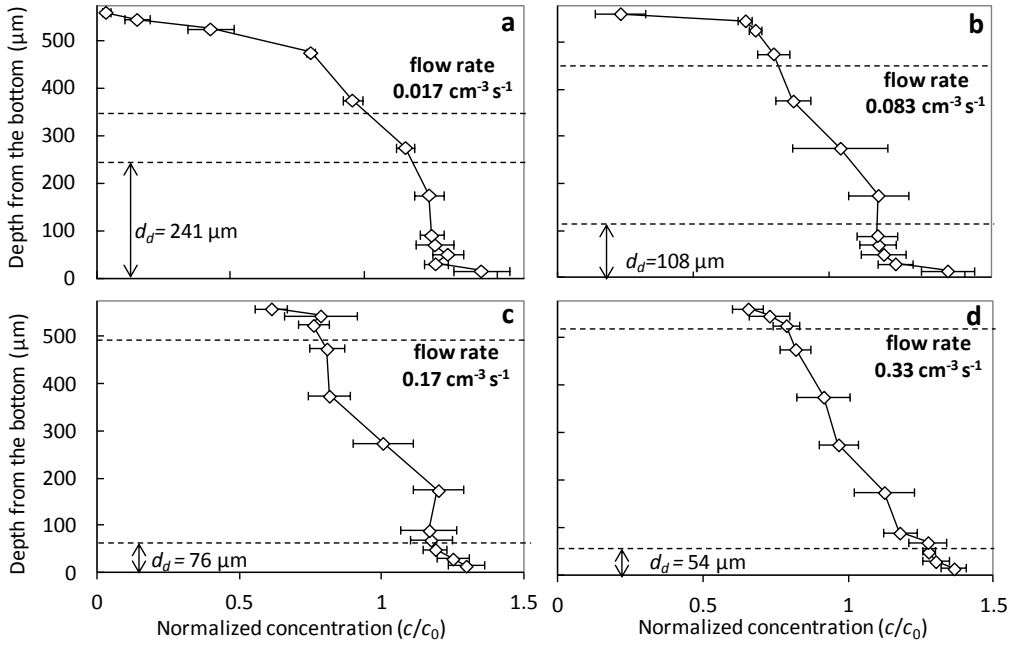

Figure 3. Height dependence of the bacterial concentration at different flow rates at 8.2 cm from the entrance of the PPFC measured 20 min after recirculation of the bacterial suspension, and normalized with respect to the original staphylococcal concentration c_0, in the suspension (3×10^8 cm^{-3}). Dotted lines indicate the position of the diffusion boundary layer as calculated from Eq. (9).

Bacterial concentrations along the height of the PPFC at 8.2 cm from the chamber entrance and normalized with respect to c_0 are shown in Fig. 3. Toward the top plate, bacterial concentrations are lower than overall in suspension, while

bacteria accumulated toward the bottom plate. Flow rate has a marked influence on the height dependence of the bacterial concentration. Higher flow rates resulted in more homogeneous and symmetrical bacterial concentration profiles than lower flow rates.

Bacterial concentration under stagnant conditions were measured as a function of time at 325, 375 and 425 μm above the bottom plate of the PPFC (Fig. 4). The sedimentation velocity of *S. aureus* in PBS buffer at room temperature was subsequently calculated from Eq. 5 to be 240 ± 12 μm h^{-1}.

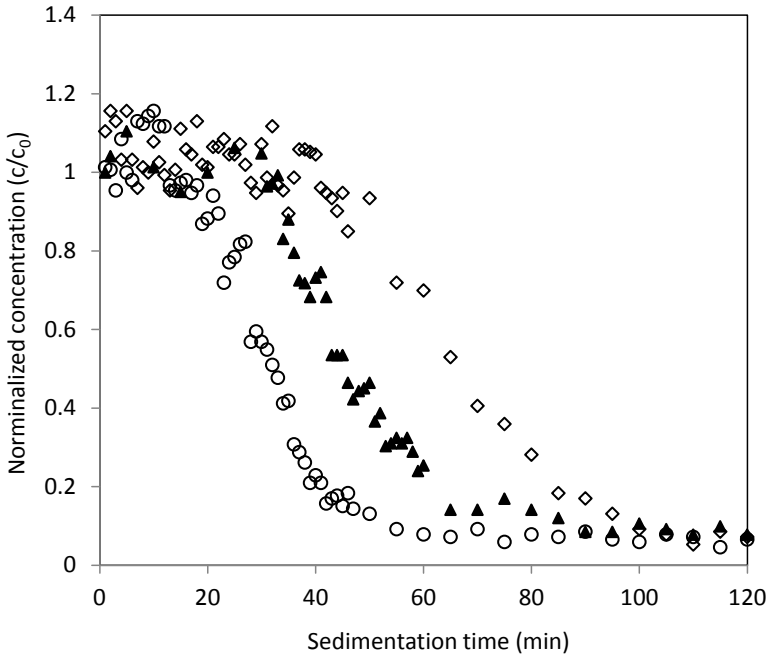

Figure 4. Bacterial concentrations at various heights (○:425 μm, ▲:375 μm and ◇: 325 μm) in the PPFC under stagnant conditions as a function of time. The bacterial concentration was normalized with respect to the original bacterial concentration in suspension, c_0 (3×10^8 cm^{-3}).

Deposition rates due to sedimentation and diffusion

Based on the bacterial concentration height profiles and sedimentation velocities calculated, the contributions of sedimentation and diffusion toward mass transport to the bottom plate of the PPFC were calculated (Fig. 5) for a distance of 8.2 cm from the entrance of the channel. The contribution of sedimentation toward mass transport ranges from 2700 to 3300 cm^{-2} s^{-1} and decreases slightly with increasing flow rate. The diffusional contribution to mass transport rates calculated at the same level, ranges from -27 to -120 cm^{-2} s^{-1} (i.e. directed towards the bulk fluid) for the various flow rates.

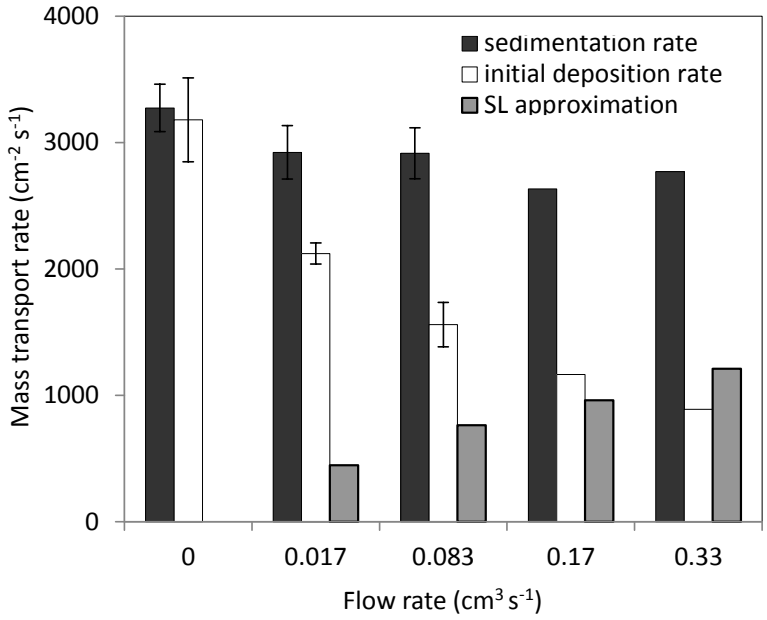

Figure 5. Experimentally determined sedimentation rates, j_s, and initial deposition rates to the bottom plate, j_0, together with theoretical deposition rates, j_0^* based on the Smoluchowski–Levich (SL) equation.

DISCUSSION

A five-fold difference in the initial staphylococcal deposition rate between the bottom and top plates of the PPFC (Fig. 1) indicated that a different mass transport mechanism is operative for the bottom and top plates. This difference is not accounted for by a convective-diffusion model neglecting interaction forces and gravity, since convective-diffusion assigns equal mass transport to the top and bottom plate. In order to experimentally determine the contribution of sedimentation to the mass transport in a PPFC, a microscopy-based method was introduced to measure the height-dependent bacterial concentration, sedimentation velocity, and the sedimentation rate. The sedimentation velocity of micron-sized bacteria can also be theoretically calculated based on a free sedimentation model applying Stokes' law, as given by

$$v_s = \frac{2}{9\eta}(\rho_s - \rho_f)gr^2 \qquad (10)$$

with ρ_s the mass density of bacteria taken as 1.100 g cm^{-3} [20], and g the acceleration of gravity (9.8 m s^{-2}). Application of Eq. 10 results in a sedimentation velocity of 264 μm h^{-1}, which compares well with the experimental sedimentation velocity obtained here for *S. aureus* ATCC 12600, and is comparable with the sedimentation rate of 296 μm h^{-1} for *Arthrobacter* B672 in water, determined elsewise [20].

Bacterial concentrations as a function of height showed that bacteria are absent in the upper part of fluid and accumulate in the lower part of the channel due to sedimentation (Fig. 3). Interestingly, there is no decrease in bacterial concentration towards the surface, expected to occur within the diffusion boundary layer, but rather an increase due to sedimentation (see Fig. 3). As a

result, diffusion near the bottom plate is directed towards the bulk fluid. The comparsion of the experimentally determined initial deposition rates with the mass transport due to sedimentation and convective-diffusion according to the SL-approach (Fig. 5) indicate that sedimentation is the dominant mass transport process in the PPFC within the range of flow rates applied in this study. Note that the experimentally determined initial deposition rate and the sedimentation rate determined are similar under stagnant conditions, even though electrostatic interactions are repulsive. Likely, bacteria have enough time under stagnant conditions to adhere on electrostatically favorable spots on the substratum surface. These results support the validity of the assumptions made in the derivation of Eq. 5 that diffusional transport far from the collector surface is negligeable, as compared to mass transport by sedimentation. From Fig. 5 it can also be seen that deposition efficiencies of *S. aureus* ATCC 12600 exceed unity by a factor of 2.0 to 4.7 for intermediate flow rates, while being close to unity at more elevated flow rates. Under flow conditions, electrostatic repulsion and shear forces apparantly prevent bacteria to deposit directly on arrival. However, calculated deposition efficiencies, j_0 / j_0^*, on basis of

$$j_0^* = j_s(d_f) = c(d_f) \cdot v_s \tag{11}$$

always yielded values lower than unity. Although this does not rule out all previous assumptions that surface appendages on bacterial cell surfaces may positively contribute to bacterial mass transport, it seems more realistic to calculate bacterial deposition efficiencies in a PPFC with respect to sedimentation rates rather than with respect to convective-diffusional mass transport. It has also been suggested to account for sedimentational mass transport in a PPFC by

averaging initial deposition rates for the top and bottom plate [18], but for the present strain and substratum this still yields deposition efficiencies with respect to the SL approach larger than unity (2.6 and 1.2 at flow rates of 0.017 and 0.084 $cm^3\ s^{-1}$, respectively).

When accounting for sedimentation in calculating deposition efficiencies, it must be realized that deposition efficiencies decrease from 0.97 under stagnant conditions to 0.36 at a flow rate of 0.33 $cm^3\ s^{-1}$ and also decrease with increasing distance from the entrance of the flow chamber (see Fig. 5). This flow rate and distance dependence can be explained by considering a steady flow with constant bacterial concentrations over the entire volume of the chamber. Not all bacteria sedimenting to the bottom plate will adhere firmly, as indicated by the deposition efficiencies smaller than unity, which is due to blocking or shear forces acting upon bacteria in the flow [21]. Consequently, these non-adhering bacteria will be carried along the surface by the flow, yielding an increase in bacterial concentration near the surface and an increased deposition rate at larger distances, *x*, from the entrance of the flow chamber. Note that this effect gets even more pronounced for lower flow rates.

CONCLUSION

A microscopic method was introduced to experimentally determine the contribution of sedimentation towards bacterial mass transport in a PPFC. Sedimentation, rather than convective-diffusion, turned out to be the major mass transport mechanisms in the PPFC, as illustrated here for *S. aureus* ATCC 12600. This explains why bacterial deposition efficiencies calculated with respect to the SL-approximate solution of the convective-diffusion equation are in excess of

unity, and it is proposed that deposition efficiencies in a PPFC are calculated with respect to the rate of sedimentation. Sedimentation rates however, can be dependent on the flow rate and distance from the flow chamber entrance, which can be easily accounted for when employing the proposed method to calculate the contribution of sedimentation to mass transport in a PPFC.

REFERENCES

[1] De Kerchove A., Elimelech M., (2007) Impact of alginate conditioning film on deposition kinetics of motile and nonmotile *Pseudomonas aeruginosa* strains*, Appl. Environ. Microbiol.* **73** 5227-5234.

[2] Hu J. Y., Yu B., Feng Y. Y., Tan X. L., Ong S. L., Ng W. J., Hoe W. C., (2005) Investigation into biofilms in a local drinking water distribution system, *Biofilms* **2** 19-25.

[3] Li Q., Logan B. E., (1999) Enhancing bacterial transport for bioaugmentation of aquifers using low ionic strength solutions and surfactants, *Water Res*. **33** 1090-1100.

[4] Xu L. C., Logan B. E., (2005) Atomic force microscopy colloid probe analysis of interactions between proteins and surfaces, *Environ. Sci. Technol.* **39** 3592-3600.

[5] Davies D., (2003) Understanding biofilm resistance to antibacterial agents, *Nat. Rev. Drug Discov.* **2** 114-122.

[6] Thomas W. E., Trintchina E., Forero M., Vogel V., Sokurenko E. V., (2002) Bacterial adhesion to target cells enhanced by shear force, *Cell* **109** 913-923.

[7] Walker S. L., Hill J. E., Redman J. A., Elimelech M., (2005) Influence of growth phase on adhesion kinetics of *Escherichia coli* D21g, *Appl. Environ. Microbiol.* **71** 3093-3099.

[8] Munn L. L., Melder R. J., Jasin R. K., (1994) Analysis of cell flux in the parallel plate flow chamber: Implications for cell capture studies, *Biophys. J.* **67** 889-895.

[9] Garrett T. R., Bhakoo M., Zhang Z., (2008) Characterisation of bacterial adhesion and removal in a flow chamber by micromanipulation measurements, *Biotechnol. Lett.* **30** 427-433.

[10] Busscher H. J., Van der Mei H. C., (2006) Microbial adhesion in flow displacement systems, *Clin. Microbiol. Rev*. **19** 127-141.

[11] Elimelech M., (1994) Particle deposition on ideal collectors from dilute flowing suspensions: Mathematical formulation, numerical solution, and simulations, *Sep. Technol*. **4** 186-212.

[12] Hogt A. H., Dankert J., Feijen J. J., (1986) Adhesion of coagulase-negative staphylococci to methacrylate polymers and copolymers, *J. Biomed. Mater. Res.* **20** 533-545.

[13] Busscher H. J., Bellon-Fontaine M. N., Mozes N., Van der Mei H. C., Sjollema J., Cerf O., Rouxhet P.G., (1990) Deposition of *leuconostoc mesenteroides* and *streptococcus thermophilus* to solid substrata in a parallel plate flow cell, *Biofouling* **2** 55-62.

[14] Van der Mei H. C., Brokke P., Dankert J., Feijen J., Busscher H. J., (1992) Influence of electrostatic interactions on the deposition efficiencies of coagulase-negative staphylococci to collector surfaces in a parallel plate flow chamber, *J. Dispersion Sci. Technol.* **13** 447-458.

[15] Van Oss C. J., Interfacial forces in aqueous media, Marcel Dekker, New York, 1994.

[16] Hermansson M., (1999) The DLVO theory in microbial adhesion, *Colloids Surf B: Biointerfaces* **14** 105-119.

[17] Das T., Sharma P. K., Busscher H. J., Van der Mei H. C., Krom B. P., (2010) Role of extracellular DNA in initial bacterial adhesion and surface aggregation, *Appl. Environ. Microbiol.* **76** 3405-3408.

[18] Boks N. P., Norde W., Van der Mei H. C., (2008) Busscher H. J, Forces involved in bacterial adhesion to hydrophilic and hydrophobic surfaces, *Microbiology* **154** 3122-3133.

[19] Levich V. G., Physicochemical hydrodynamics. Prentice-Hall Inc., New Jersey, 1962.

[20] Wan J., Tokunaga T. K., Tsang C. F., (1995) Bacterial sedimentation through a porous medium, *Water Resource Res*. **31** 1627-1636.

[21] Dabros T., Van de Ven T. G. M., (1982) Kinetics of coating by colloidal particles, *J. Colloid Interface Sci.* **89** 232-244.